Dyes removal from textile wastewater by agricultural waste as an absorbent – A review

Farah Amalina[a], Abdul Syukor Abd Razak[a], Santhana Krishnan[b], A.W. Zularisam[a], Mohd Nasrullah[a,*]

[a] Faculty of Civil Engineering Technology, Universiti Malaysia Pahang (UMP), Lebuhraya Tun Razak, Gambang, 26300 Kuantan, Pahang, Malaysia
[b] Department of Civil and Environmental Engineering, Faculty of Engineering, Prince of Songkla University, Songkhla 90110, Thailand

ARTICLE INFO

ABSTRACT

Water pollution from the textile industry affects environmental conditions by generating large-scale effluent mixed with various dyes. Dyes are mostly organics with multiple compound structural and molecular weight variations; if not managed properly before release, they may harm the environment and organism. However, many dyes are categorized into distinct groups, and various adsorbents for dye adsorption have been identified. Among these dyes, methyl dyes, which come in multiple colours, are the most popular in research due to their availability and accessibility. It is imperative to use effective treatments using special adsorbents to remediate water contamination before discharging into streams. As awareness of environmental issues increases with time, the need for a wide range of adaptive alternative feedstock that satisfies ecological regulations has become a priority for researchers worldwide. Therefore, there is a need to develop other adsorbents from alternatively economic raw materials such as locally available industrial and mineral waste and by-products. Additionally, numerous materials have been used, prepared, or grafted from various agricultural peel-based adsorbents. Biomass is a significant source of renewable adsorption processes for hazardous compounds, including toxic organics and metals/elements. It is much cheaper, has abundance, effective adsorption capability, and reusability, have numerous advantages over conventional materials. This review focuses on using plant agricultural wastes to remove dyes. Different adsorption capacities, operating conditions, and application forms have been investigated. The adsorption kinetics and isotherms are demonstrated to illustrate the adsorbent's properties and adsorption mechanisms.

1. Introduction

The textile sector is among the largest industries in the world, yet it emits high levels of dyes, hazardous metal components, and chemicals in discharged wastewater (Kadhom et al., 2020). Textile wastewater effluents are hazardous wastes containing toxic complex elements, if not properly handled, may harm the environment, destroying aquatic ecosystems and human health (Ahmed et al., 2020). Pollutants from dye wastewater block ecosystems from performing their functions required by communities and threaten environmental sustainability (Amalina et al., 2021; Li et al., 2019). Pollution caused by the textile dyeing industry due to the intense colour of the wastewater discharges cannot be hidden, which is persistent due to the poor biodegradability of these dyes (Hassan and Carr, 2021).

Over 100,000 dyes are reported to be useable, with the textile industry being the primary application (Amalina et al., 2022c). As a result, it is exp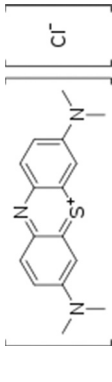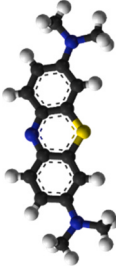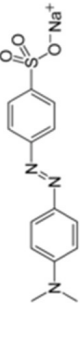e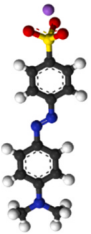cted that more than 300,000 tonnes per annum will be discharged into the waterways from the textile industry, excluding other sectors (Kadhom et al., 2020). The main characteristics of these effluents include higher levels of alkaline content, biological oxygen demand (BOD), chemical oxygen demand (COD), and total dissolved solids (TSS) with a concentration of dye/dm^3 below 1 g (Jesudoss et al., 2020). Adverse effects of dyes on plants and animals include skin irritation, carcinogenesis, decreased photosynthesis in aquatic plants, and disturbing the exquisite balance of the ecosystem (Amalina et al., 2019; Bagotia et al., 2020).
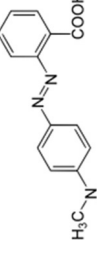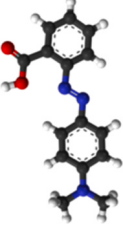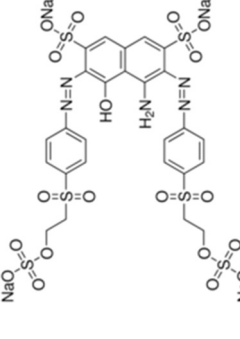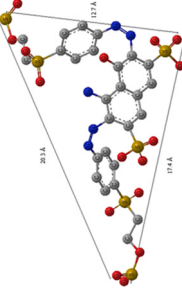
Dyes used in textiles are classified into two types, natural and synthetic dyes. Prior to the middle of the 19th century, dyes were derived from raw materials such as beet root. Typically, natural dyes are derived from plant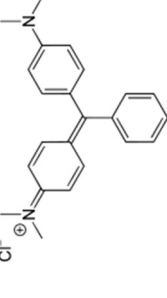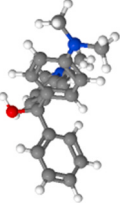s, insects/animals, and minerals (Amalina et al., 2022d). They are generally less allergic and poisonous than synthetic dyes and produce biodegradable effluent (Benkhaya et al., 2020). Synthetic dyes are typically categorized as per their use, chemical structure, ionic forms, solution state, and colour (Chen et al., 2019).

---

* Corresponding author.
  E-mail address: nasrul.ump@gmail.com (M. Nasrullah).
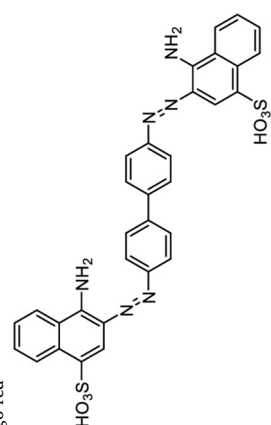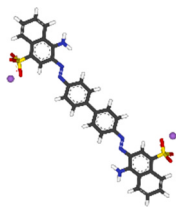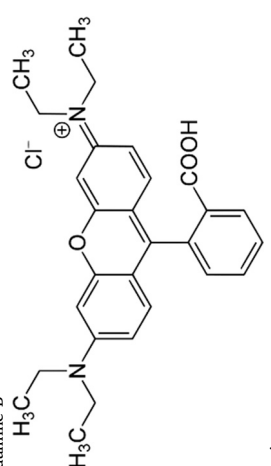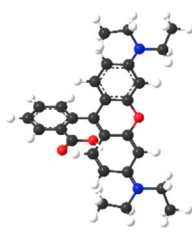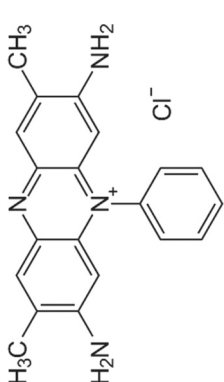
Table 1

Organic dyes and chemical molecular structure for adsorptive removal by an adsorbent.

Name and Chemical Structural	Structural Model	Formula	Molar Mass (g/mol)	Density (g/cm³)	Ref.
Methylene blue		$C_{16}H_{18}ClN_3S$	319.85	0.98	(Yoneda et al., 2021)
Methyl orange		$C_{14}H_{14}N_3NaO_3S$	327.33	1.28	(Labiadh and Kamali, 2020)
Methyl red		$C_{15}H_{15}N_3O_2$	269.304	0.791	(Roik et al., 2021)
Malachite green		$C_{23}H_{25}N_2$	364.911	1.0448	(Nazir et al., 2021)
Reactive Black 5		$C_{26}H_{21}N_5Na_4O_{19}S_6$	991.8	1.21	(Lai et al., 2020)

Table 1 (*continued*)

Name and Chemical Structural	Structural Model	Formula	Molar Mass (g/mol)	Density (g/cm^3)	Ref.
Congo red		$C_{32}H_{22}N_6Na_2O_6S_2$	696.665	0.995	(Stjepanovi et al., 2021)
Rhodamine B		$C_{28}H_{31}ClN_2O_3$	479.02	0.79	(Saigl and Ahmed, 2021)
Safranin		$C_{20}H_{19}ClN_4$	350.85	0.98	(Mukhlish et al., 2020)

The most effective method for organizing dyes is their chemical structure, which provides numerous advantages (Nyoo et al., 2021). Synthetic dyes are formulated to meet current biological and physical resistant colouring agent requirements (Zubair et al., 2021). Thus, synthetic dyes are being established and gradually replacing natural dyes, especially in the textile and fabric industries (Zhou et al., 2019).

Generally, synthetic dyes contain several dyes in each category, including anionic, cationic, and non-ionic (Amalina et al., 2022c). Anionic dyes include direct, reactive, and acid dyes; cationic and non-ionic dyes include base and dispersed pigments, respectively (Kadhom et al., 2020). For instance, methylene blue is a widely used dye in the textile sector and other chemicals, medicinal, and biological applications (Nedjai et al., 2021). Methylene blue is a cationic stain with a complex structure, making it challenging to remove. Similarly, methyl orange is used in numerous industries and has the same molecular weight as methylene blue (Rattanapan et al., 2017). The molecular structure of the multiple dyes is depicted in Table 1. In addition to methyl orange, methyl red is an azo dye with considerable molecular weight and numerous barriers to remove; many additional acidic and basic dyes exist and must be discarded.

Multiple decontamination techniques, including filtration, chemical oxidation, chemical coagulation, precipitation, electrochemical removal and electrocoagulation, photocatalysis, ultrasonic and biological decomposition, and adsorption, are employed for dyes removal (Krishnan et al., 2021a, 2021b; Nasrullah et al., 2020). Among these, adsorption offers numerous advantages due to its easy and direct operation, high efficiency, simplicity, and lack of dangerous by-products (Amalina et al., 2022a, 2022b). When the strengths and disadvantages of each technique are examined, adsorption may be a perfect idea; hence, numerous research organizations have reported on it extensively (Jinendra et al., 2021; Nasrullah et al., 2022).

Adsorbents are the primary factor in adsorption, for which many substances have been utilized (Amalina et al., 2022e). Moreover, natural adsorbents are highly effective (Ahmed et al., 2020), and scientific researchers have recently attracted attention. The advantages of adsorption are simplicity, efficient, high selectivity, high performance, inexpensive recovery of adsorbent and adsorbate, and efficient removal of contaminants (Nwuzor et al., 2018; Zhou et al., 2019). For instance, activated carbon (AC) is widely reported in the context of dyes and organics adsorption due to its exceptional performance in this area, yet its relatively high cost limits its application. Therefore, natural resources such as adsorbents derived from agriculture are more alluring, as their efficacy for various dye adsorption types is well-established (Nasrullah et al., 2019; Zaied et al., 2020). Multiple techniques have been used to modify adsorbents, which have proven highly effective in enhancing adsorption (Esteves et al., 2020).

In recent times, academic researchers have shown a growing interest in developing economical and environmentally friendly adsorbents for wastewater treatment. Modern studies have discovered a variety of inexpensive adsorbents produced from agricultural waste that is currently being explored for the removal of dyes from wastewater. Today, agricultural peels-based adsorbents have validated their potential as eco-friendly and cost-effective, readily available (because all inhabited areas generate biowaste), efficient, and might be utilized in the development of absorbent material for addressing the water contamination issue (Amalina et al., 2020; Haziq et al., 2020). The direct use of developing, functioning, and/or synthesizing adsorbents constitutes the application of this resource in the adsorption process (Bedia et al., 2018; Iftekhar et al., 2018). This review examines how locally available agricultural wastes can be converted to the respective carbonized (charcoal) or activated carbon and biochar forms. The schematic in Fig. 1 depicts the utilization of plant waste in dye removal.

In this study, the authors present a range of studies on removing the most often reported dyes utilizing green materials, mainly agricultural waste, especially peels, leaves, and seeds. This waste was used in various ways, particularly as a raw material for synthesizing modified adsorbents. The adsorption capacity, isotherm, influencing factors, efficiency, etc., were described to comprehend this material's most prevalent behaviours and characteristics. This study provides a current overview of the use of biomasses as adsorbents for removing dyes, where different adsorption results were documented.

2. Dyes removal using agricultural waste

The expansion of the textile industry resulted in the discharge of vast volumes of effluents containing dye. This dye is harmful to humans and organisms, even in extremely low doses (Mishra et al., 2021). Methylene blue, orange, red, and yellow dyes have also been used commercially (Tkaczyk et al., 2020; Zhu et al., 2018). Various researchers have analysed the potential of agricultural waste biomass as an adsorbent for wastewater treatment and have found encouraging results that minimize the harmful effect of colours on aquatic systems (Amalina et al., 2022f; Shamsollahi and Partovinia, 2019).

Agricultural residues have been proposed as low-cost alternative adsorbents due to their high proportion of cellulose and lignocellulose (Aguilar-Rosero et al., 2022). Agricultural waste is classified as crop and processing residues (Raud et al., 2019). Cereals, seeds, fruits, vegetables, herbage, and forage, which represent the most common wastes in the food and agricultural industries, have enormous potential as adsorbents capable of decontaminating polluted effluents (Ibrahim and Maslehuddin, 2020). On the other hand, products or by-products, including bran, husk, citrus peel, onion peel, garlic peel, shells, etc., are produced during processing residues (Senthil and Lee, 2020). Variety types of agricultural and plant wastes are selected as inexpensive by-products to remove various dyes from aquatic solutions (Nyoo et al., 2021). Agricultural waste products have many advantages, such as ease of disposal, high biodegradability, low price, high availability, and sustainable and environmentally friendly wastewater treatment (Krishnan et al., 2021a, 2021b; Liu et al., 2018). It is noted that the maximum absorption capacity of crop residue is ecologically sustainable, economically viable, and technically feasible for long-term industrial use. Since scientists discovered the adverse effects of dyes, almost every physical, chemical, and biological system for treating dyeing wastewater had been used, especially coagulation/flocculation, membrane separations, adsorption, ion exchange, advanced oxidation, and electrochemical processes (Krishnan et al., 2021a, 2021b; Mohamad et al., 2022; Zaied et al., 2020).

2.1. Removal of methylene blue

Methylene blue (MB) is the most persistently utilized dye as a standard for microfiltration and absorption studies (Kadhom et al., 2020). Its molecular weight made it suitable for numerous uses, particularly medical ones. MB, a large heterocyclic aromatic dye, is an excellent option for evaluating the adsorbent's efficiency, whose mesoporosity means that it may be used to adsorb liquid pollutants (Gu, 2021). Thus, the MB value is the most used parameter to accurately calculate the adsorption potential of AC's mesoporous structure. Nevertheless, MB is formulated as ($C_{16}H_{18}N_3SCl$); if not adequately treated before release, it can harm the ecosystem. It has been observed that high dosages of MB can directly oxidize haemoglobin and produce methemoglobinemia. Additionally, it can cause haemolysis-related complications, particularly in neonates. Long-term exposure may cause serious anaemia (Kadhom et al., 2020; Wahi et al., 2017).

Üner et al. (2016) widely employed watermelon rind (WMR) for the chemical activation of AC (WRAC) utilizing zinc chloride ($ZnCl_2$). The author has conducted a comprehensive investigation of the adsorption of MB using AC derived from WMR and obtained excellent findings. When the adsorption temperature increased, MB's maximal adsorption capacity (qm) was determined to be 231.48 mg/g. The Langmuir isothermal and pseudo-second-order (PSO) models best fit the equilibrium and kinetic data. The authors investigated several models for defining
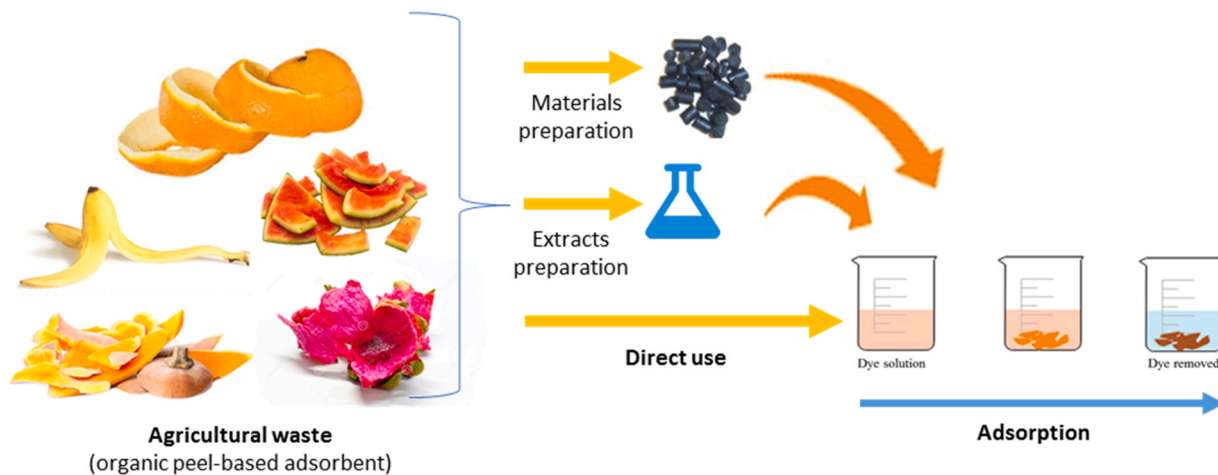
Fig. 1. A general diagram shows methods of using agriculture waste in dye removal.

the diffusion mechanism for MB adsorption into WRAC, including the intraparticle diffusion model, the bangham model, and the Boyd model. The authors found that intraparticle, film, and pore diffusion played a significant role in adsorption. Üner et al. (2016) also conducted a thermodynamic analysis of the adsorption process and reported that it was spontaneous, endothermic, and governed by the physisorption mechanism. Sahu et al. (2020) reported the same findings while removing MB with kendu fruit peel. The WMR's carbonization temperature was 700 °C using thermogravimetric and BET analyses (Üner et al., 2016). The pores were empty before MB adsorption. After MB adsorption, the pores were filled with MB molecules, and MB covered the surface of WRAC in solution. At 303 K, the chemically activated WMR demonstrated a higher adsorption capacity (200 mg/g) than the WMR (188.68 mg/g). The kinetic and equilibrium data for both adsorption processes were comparable, as both data sets fit the PSO model and Langmuir isotherm. Jawad et al. (2019) determined that the process was spontaneous and endothermic and followed the physisorption mechanism. In the case of non-activated WMR, however, physisorption predominated, which is compatible with the results of Üner et al. (2016) and Bhattacharjee et al. (2020a, 2020b). In all cases, adsorption uptake increased with increasing pH, and the initial, unadjusted pH of 5.6 was appropriate. In both instances, the researchers determined that WMR functional groups, such as carboxyl and hydroxyl, played a crucial role in the MB biosorption process. Both Üner et al. (2016) and Jawad et al. (2019) performed chemical activation of the melon rind using ZnCl$_2$ and sulfuric acid (H$_2$SO$_4$) and discovered the adsorption mechanism to be endothermic, which indicates significant surface structure changes in the adsorbent as a result of chemisorption.

Biodegradable wastes were utilized to absorb the MB. Rashid et al. (2019) produced AC from pumpkin peels that were functionalized by various extracts and utilized to absorb the dye from aqueous solutions. The peels were carbonated at 250, 350, 450, and 550 °C, with 250 °C being the most effective. For AC production, as the temperature increases, the structure may shrink the absorption sites together (Rashid et al., 2019). AC was treated using beetroot extract, citric acid, nitric acid, and oxalic acid; the beetroot gave the best performance among these agents. Under an initial concentration of 0.2 g/L, an adsorbent amount of 0.5 g/L, a temperature of 50 °C, and 180 min, the maximum adsorption capacity was 198.15 mg/g. This increase in adsorption capacity can be explained by the fact that when heat is applied and aromatics evaporate, the carbon network expands as the existing pores expand and new pores form. The adsorption kinetics followed a pseudo model of the second order; additionally, the equilibrium data show a better fit with the Langmuir model than with the Freundlich model, which describes a monolayer adsorption process.

The banana peel produced porous AC using the hierarchically interconnected approach, followed by hydrothermal treatment and KOH activation (Saigl and Ahmed, 2021). Hierarchically interconnected porous AC have high specific surface areas, vast numbers of dye adsorption sites, and interconnected pores enabling dye molecule dispersion and transport (Lu and Li, 2019). This structure generates a framework with a high surface area (approximately 600 m^2/g with an average pore diameter of 2.11 nm and a pore volume of 0.32 cm^3/g), which enhances the transport and diffusion of the dye within the AC and increases the adsorption sites. By increasing the dosage of the adsorbent, the dye removal efficiency improved until it reached almost 100% at a dosage of 1.5 g/L. In adsorption, the pollutant is generally removed at a fast rate and then starts to slow down until it reaches a steady state. This could initially be attributable to the availability of adsorption sites; when these become occupied, the adsorption rate decreases. It was determined that the Langmuir adsorption model best describes adsorption, while the PSO model describes adsorption kinetics. As an adsorbent for MB and other colours, the synthesis of AC from biomass has been extensively described.

Grape peel was also used in MB adsorption, applying the microwave-hydrothermal technique to treat the peel for 3 min at 180 °C (Ma et al., 2018). Despite the apparent ease of achieving these conditions, the resulting product is superior to the conventional hydrothermal procedure, which requires 16 h of treatment. Based on the Langmuir model, the optimal operating parameters for obtaining the highest adsorption capacity (216 mg/g) were a pH of 11 and an adsorbent dosage of 250 g/L. The cationic charge of MB was linked to the increased adsorption at high pH values. This strategy offers great potential because the adsorbent is economical, environmentally friendly, and effective.

The synthesis of hydrogels from the peel of pitahaya (dragon fruit) was performed using microwave (MV) radiation and compared to gamma (G) radiation (Abdullah et al., 2018). Pectin was removed from the peels and treated with acrylic acid to create polymerized hydrogels that varied according to the radiation intensity and pectin/acrylic acid ratio. Both gels contained the COO$^-$ group responsible for the dye's absorption. The optimal conditions for preparing the swelling gel were a pH of 8, a pectin/acrylic acid (Pc/AA) ratio of 2/3, and MV and gamma radiation powers of 400 W and 10 kGy, respectively. At an initial dye concentration of 20 mg/L, pH of 8, and adsorbent dosage of 20 mg, the most incredible removal efficiency was attained, which was 45%. SEM gives information on the hydrogel's pore geometry and size. Both characteristics are crucial in defining the adsorption characteristics. In contrast, Pc/AA(Mw) has a denser porous network, which may impact its absorption capacity. The presence of a crosslinking agent made the space denser, decreasing the pore size. Greater pore size minimizes the time required to attain an equilibrium.

Jawad et al. (2018) also used dragon fruit peels for MB removal, but without other treatments. The results of the Langmuir isotherm model fitted with the adsorption capacity are superior to those of the Freundlich model, whose maximum value was 192.31 mg/g. At a dosage of 600 mg/L of adsorbent, a temperature of 25 °C, an initial dye concentration of 100 mg/L, a rotating speed of 120 strokes/minute, and a contact time of 180 min, the removal efficiency was optimized to approximately 83%.

Soto-Robles et al. (2017) utilized *Lycopersicon esculentum* (tomato) peel extracts to produce modified zinc oxide (ZnO) from zinc nitrate for MB removal. As a stabilizing and reducing component, the concentration of removal influenced the form and size of zinc oxide particles. Increasing the extract concentration by 1%, 2%, and 4% caused the ZnO band gap to increase to 3.08, 3.1, and 3.18 eV and the particle diameter to rise to 6.54, 10.75, and 24 nm, respectively. MB was absorbed by 92% after 120 min and 97% after 150 min of exposure to a 4% ZnO extract concentration; this finding is greater than the impact of conventional ZnO. The results were obtained using a 4% extraction because minuscule particles were produced.

Ren et al. (2018) used pomelo peel that had been treated with citric acid ($C_6H_8O_7$) to remove MB. The removal efficiencies of MB onto pomelo peel and modified pomelo peel in averaged were 81.7 mg/g and 199.2 mg/g, respectively, implying that applying anionic groups enhanced adsorption capacity. The biosorption process was aided by increasing the dye concentration and pH of the colour solvent. On modified pomelo peel, the adsorption equilibrium took about 3 h. Treatment with $C_6H_8O_7$ was reported to have improved surface cleanliness. Furthermore, if the pH is more significant than 5.3, the charge dominates absorption, with the negative charge of the treated peels increasing absorption. The PSO model best defined the kinetics adsorption, while the Langmuir model best explained the isotherm of adsorption. The mechanism was exothermic and random and showed entropy reduction.

Said et al. (2020) investigated the synthesis of hydrochar from the male oil palm flower (MOPF) and its application for MB removal. MOPF was turned to hydrochar at 180 °C for 8 h in an oxygen atmosphere. The produced hydrochar indicated favorable properties concerning the functional group active sites, surface area, texture, and structure. The adsorption mechanism was more suitable for the monolayer Langmuir isotherm with a maximum adsorption capacity of 42.92 mg/g at 30 °C. A kinetic investigation revealed that MB adsorption followed the PSO model, demonstrating that chemisorption was the rate-determining step for MB adsorption onto hydrochar.

Peels of *Cucumis sativus* (cucumber) were employed as an MB adsorbent (Shakoor and Nasar, 2017). The best removal efficiency reached 85% at 6 g/L when the adsorbent dosage was 6 g/L; subsequent dosage increases resulted in a slight improvement in removal efficiency. Nonetheless, as the adsorbent dosage increased, the adsorption capacity dropped. After 1 h of contact, the equilibrium adsorption capacity was obtained for all initial concentrations. The removal efficiency increased with increasing pH; as a result, it reached 80% at pH 9 and higher. Entropy and enthalpy were negative; thus, as the temperature increased, the process rate slowed. In detail, utilized peels were regenerated with HCl, and the desorption efficiency was 63.6%. The Freundlich model explains the adsorption isotherm, which refers to the heterogeneous surface of the adsorbent, and the PSO model fits the adsorption kinetics.

Biochar was produced from the leaves of the Magnolia grandiflora tree and used to remove MB (Ji et al., 2019). The leaves were washed, dried, and carbonized in the furnace at 500 °C to prepare the biochar. Increasing the pH and ionic strength enhanced the adsorption capacity and removal performance. The maximum adsorption capacity at ambient temperature, pH 12, and 0.1 M ionic strength was 101.27 mg/g. The study of the thermodynamics of the process revealed that it is spontaneous and endothermic. The best models for describing the adsorption isotherm and kinetics were the Langmuir and PSO models, respectively.

In addition, Rawat et al. (2019) and colleagues investigated the removal of MB from an aqueous medium via biochar. The plant biochar was produced from Mentha plant waste by slow pyrolysis at temperatures 450 and 700 °C. It was discovered that the adsorbent synthesized at 700 °C had a significantly larger adsorption capacity (588 mg/g) than that synthesized at a lower temperature (87 mg/g). Furthermore, it has been observed that the optimal pH for maximum adsorption capacity at both temperatures was 10, which could be related to the increase in the hydrated ionic radius and the negative charge on the surface.

Cress seed mucilage was employed to produce nanoparticles of iron oxide with remarkable magnetic properties and adsorption capacity (Allafchian et al., 2019). The thermodynamic test revealed that the process was spontaneous and exothermic. The adsorption rate improved with increasing initial concentration and pH but dropped with increasing feed temperature and ionic strength. The Langmuir model determined that the maximal adsorption capacity of MB was 44.6 mg/g and its removal effectiveness was 84%. Used nanoparticles were regenerated by dispersing them in a 0.5 M aqueous HCl solution for two hours. Nonetheless, after reusing the nanoparticles, a loss in efficiency of around 52% was seen after five cycles.

Wijaya et al. (2020) employed kaffir lime peels as a green reduction agent of graphene oxide (GO) and then examined its adsorption ability for MB removal. The optimal ratio of kaffir lime peels to GO was determined to be 1:2, whereas the optimal reduction time was 8 h. The highest adsorption potential (qmax) was 276.06 mg/g. The isotherm analysis showed that MB adsorption best fit the Langmuir isotherm, whereas the kinetic study revealed that MB adsorption followed the PSO model. This method has several benefits, including simple production, a sustainable and environment-reducing agent, and non-toxic wastes at the end of the reduction process.

Hassan et al. (2020) reported using palm bark and eucalyptus biomass as adsorbents to remove MB from an aqueous solution. The carbonaceous structure of adsorbents is the main component of carbon in the biochar. Biochars from palm bark and eucalyptus have surface areas of 2.46 and 10.35 m^2/g, respectively. The mesoporous was identified by pore diameters of 4.75 and 2.29 nm. The PSO adsorption kinetic model better explained MB sorption by biochars. The Langmuir model accurately represented the MB adsorption onto biochars compared to the Freundlich adsorption isotherm model. Thomas et al. (2019) activate the sawdust carbon produced from the H_2SO_4, significantly improving MB's removal capacity.

MV biochar has also been stated to be an efficient dye remover. Li et al. (2019), who studied on orange peel reported the removed of MB by potassium carbonate (K_2CO_3) concentration on the MV biochar. The optimum adsorption of MB was 171.15 mg/g when the IR was 1.25, compared to 56.52 mg/g when the IR was 0.25. Owing to the porous structure of the char and the depletion of potassium carbonate, it is best to extract MB. The treatment expands the existent pores and creates new ones as the potassium molecule generated through oxidation spreads within the biochar's internal structure (Li et al., 2019). In another study, the MV-treated biochar empty fruit bunches showed 99.9% MB removal efficiency and 265 mg/g adsorption capacity (Daful and Chandraratne, 2018). This is due to the treated MV biochar's large surface area and pore size. Some examples of research using biomass for MB removal are provided in Table 2.

2.2. Removal of methyl orange dye

Similar to other dyes, methyl orange (MO) ($C_{14}H_{14}N_3NaO_3S$) is a hazardous substance and carcinogen (Wang et al., 2022). Exposure to MO dye can cause nausea, vomiting, and diarrhea (Eljiedi and Kamari, 2017). The removal of MO dye has been studied using various agricultural waste materials.

Zhang et al. (2020) were made of charcoal derived from pomelo peel which was then chemically activated with phosphoric acid (H_3PO_4).

Table 2
Methylene blue dye removal from textile effluent by agricultural waste as an absorbent.

Adsorbent	Activating agent	Surface area (m²/g)	Total pore volume (cm³/g) / Diameter (nm)	Adsorption rate (mg/g)	Efficiency (%)	Best Isothermal model	Best Kinetic model	Reference
Pumpkin peels	HNO_3	198.15	198.15	198.15	98	Langmuir	PSO	(Rashid et al., 2019) (Samsami et al., 2020; Yaashikaa et al., 2019)
Banana peel	CH_3COOH	600	215.7	–	100	Langmuir	PSO	(Saigl and Ahmed, 2021)
Grape peels	–	–	–	215.7	–	Langmuir	PSO	(Ma et al., 2018)
Dragon fruit peels	–	–	–	192.35	85	Langmuir	PSO	(Jawad et al., 2018)
Safflower seed	$ZnCl_2$	249.3–801.5	249.3	–	–	Langmuir	PSO	(Senthil and Lee, 2020)
Palm bark and eucalyptus	H_2SO_4	2.46 / 10.35	4.75 / 2.29	2.66 / 2.06	–	Langmuir	PSO	(Hassan et al., 2020)
Bamboo	$KHCO_3$	1425	187	401.88	87.79	Freundlich	PSO	(Singh et al., 2021)
Watermelon rind	$ZnCl_2$	500	–	231.48	98	Langmuir	PSO	(Üner et al., 2016)
Pomelo peel	H_2SO_4 / $C_6H_8O_7$	1500	–	188.68 / 199.2	85	Langmuir	PSO	(Bhattacharjee et al., 2020a) (Ren et al., 2018) (Xiang et al., 2020)
Sugarcane straw	H_2SO_4	590	–	5.5	82.78	Langmuir	PSO	(Rangabhashiyam and Balasubramanian, 2019)
Sawdust	HCl	590	–	304.2	–	Langmuir	PSO	(Thomas et al., 2019)
Orange peel	Microwave K_2CO_3	1391	0.72	171.15	–	Langmuir	PSO	(Oliveira et al., 2017) (Li et al., 2019)
Empty fruit bunches	CO_2	1300–1400	–	265	99.9	Langmuir	PSO	(Daful and Chandraratne, 2018)
Citrus pectin	$ZnCl_2$	1983	–	1155.2	–	Langmuir	PSO	(Abdullah et al., 2018)
Cotton stalks	H_3PO_4	795.84	–	85	–	Langmuir	PSO	(Danish and Ahmad, 2018)
Cucumis sativus peels	HCl	–	–	21.45	85	Freundlich	PSO	(Shakoor and Nasar, 2017)
Pitahaya peels	–	–	–	–	35	–	PSO	(Abdullah et al., 2018)
Cress seeds mucilage	–	–	–	101.27	–	Langmuir	PSO	(Allafchian et al., 2019)
Cauliflower leaf powder	–	–	–	149.00	88.1	Freundlich	PSO	(Ansari et al., 2019)
Potato Stem powder	–	–	–	41.6	82	Langmuir and Freundlich	PSO	(Gupta et al., 2016)
Potato Leaves powder	–	–	–	52.6	87	Freundlich		
Sulfonated tea waste	–	–	–	1007.61	> 99	Langmuir	PSO	(Ahsan et al., 2018)

The optimum pH and solvent dosage are reported to be 3 and 1 g/L, respectively; after investigating the contact time, pH, dye concentration, and biochar dose are all variables to consider. A residence time ranging from 0 to 300 min was examined, and absorption rate results were confirmed at 140 mg/g at 70 min. The absorption potential was proportional to the dye concentration. The findings were compared using the Langmuir, Freundlich, Temkin, and BET models; however, the Freundlich isotherm provided the best fit as opposed to the others. Besides, the PSO model represented the kinetic findings better than the first-order model.

MO can also be reduced through degradation, where nanoparticles can regulate the reaction. Prasad et al. (2017) generated Fe_3O_4 magnetic particles with a size range of 20–30 nm and a surface area of $17.6 \, m^2/g$ from an aqueous extract of *Pisum sativum* peels. UV spectroscopy investigated the catalytic degradation property in response to magnetic and other features. At a pH of 5.5, the removal efficacy reached about 96%. The dye removal rate enhanced with increasing adsorbent dosage but declined as dye concentration at the intake increased. Similarly, Karnan and Selvakumar (2016) generated ZnO nanoparticles with a particle size of 25–40 nm and a surface area of $69 \, m^2/g$ from rambutan peel extract and evaluated their ability to remove MO dye via photodegradation. Peels of *Nephelium lappaceum L.* (rambutan) served as a binder, making the method environmentally friendly. In addition, the powder was tested using various techniques, including UV visible spectroscopy, to detect dye degradation. After 120 min in the presence of UV radiation, the degradation percentage was approximately 84%. The chemical oxygen demand (COD) test revealed that mineralization was achieved, as the COD values reduced from 6162–481 mg/L.

AC was produced from biomass waste and employed to absorb MO. Tao et al. (2019) generated AC from shaddock (pomelo) peels by carbonizing at high temperatures and activating with phosphoric acid. The researchers utilized this fruit peel since it performed the best when compared to orange, apple, banana, and tangerine peels. Therefore, it was used to study the absorption of MO and Cr (VI) in single and binary-component systems (Fang et al., 2021). In a system with a single component, the highest dye adsorption capacity exceeded 94.6 mg/g at pH 3, and the Freundlich model was used to explain the dye sorption. The extended Freundlich multicomponent isotherm was discovered to better apply to the binary system. In the binary system, it was found that dye adsorption lowered chromium adsorption, whereas chromium presence did not affect dye adsorption. The high acting force between the AC and the dye was attributed to the dye's high adsorption capacity. Similarly, Kadhom et al. (2020) synthesized AC from walnut peels, activated it with $ZnCl_2$, and used it to remove methyl organic and acid magenta dyes. It was observed that the adsorption capacity and removal rate increase as the adsorption time and pH decrease. But, as the initial concentration of the adsorbate increases, the adsorption increases and the removal rate drops until the adsorption capacity reaches its maximum at an initial concentration of 180 mg/L of MO. After 6 h, the adsorption capacity exceeded its maximum, and at a pH of 6, 95% of these two dyes were removed. A quasi-two-dimensional equation represented the adsorption mechanism of MO and acid magenta, and the findings indicated that they were subject to monolayer and multilayer adsorption, respectively.

Pomelo peels were employed to develop porous carbon, which was then treated with KOH to absorb MO (Li et al., 2016). Findings indicate that a 2:1 ratio of KOH to pre-carbonized material provided the highest performance, with a maximum adsorption capacity of 680 mg/g. The PSO model was employed to describe the kinetics of adsorption, and the Langmuir isotherm was shown to be a better fit for the experimental data than the Freundlich model. Adsorption occurred immediately and exothermically.

Danish and Ahmad (2018) examined the performance of AC obtained from *Acacia mangium* wood towards MO dye. Using the face-centered central composite design method of response surface

methodology, batch adsorption was conducted to optimize the adsorbent dosage, temperature, and contact time for maximum adsorption capacity and percentage removal rate of MO dye. The optimal conditions for maximal adsorption capacity and removal percentage were found to be 0.51 g/L, 55.0 °C, and 24 h for a dose of AC, temperature, and contact time, respectively. At optimal operating conditions, the maximum adsorption capacity and removal percentage were reported as 181 mg/g and 90.5%, respectively. The thermodynamics and kinetics of MO dye degradation under optimal operating variable processes were investigated. It was discovered that it fitted the endothermic and spontaneous PSO kinetic rate model.

Hajialigol and Masoum (2019) used walnut peels to produce AC, which was then activated with $ZnCl_2$ and stripped of the MO and acid magena dyes. The maximum adsorption potential is achieved at a MO concentration of 180 mg/L. Once the initial concentration of the adsorbate is increased, the adsorption rises but the adsorption rate decreases. The removal potential peaked after 6 h and at a pH of 6, removing these two dyes reaching 95%. MO and acid magenta adsorption behaviour were defined by a quasi-two-dimensional equation, indicating that they were adsorbable in monolayers or multilayers, respectively.

Machrouhi et al. (2019) examined the adsorption efficacy of ACs extracted from *Thapsia transtagana* stems for removing MO dyes from the solvents. The authors found that at 500 °C for 145 min, the maximum adsorption potential was 118.10 mg/g with a 2 g/g IR. The impregnation and modification temperatures have been the most critical parameters that positively affected the activation process. Jawad et al. (2019) investigated the adsorption efficiency of nickel nanoparticles adsorbent made from *Citrullus colocynthis* (bitter cucumber) stem extract to remove the reactive yellow-160 dye. By using 0.02% dye concentration, pH 7, temperature 40 °C, and 9 mg/L adsorbent content, they achieved a maximum decolourization of 91.4%. Naik et al. (2019) applied banana pseudo-stem cellulose-based super adsorbent hydrogels via free radical graft co-polymerizing sodium acrylate and acrylamide. Authors explored the ability of super-absorbent hydrogels to dissolve MO dye and discovered that average absorption was 124 mg/g, with the greatest desorption of > 96% for both dyes, leading to a rise in hydrogel use.

Due to the presence of raw elements in the waste disposal structure, AC was often documented as a product of carbonation from agricultural waste. Commonly, the procedure entails reducing the waste to powder, followed by drying, pre-carbonation, carbonation in the presence of N_2 and a base, and acid and water washing. Table 3 lists the research on utilizing agricultural waste for MO removal.

2.3. Removal of Methyl Red Dye

Methyl red (MR) is an anionic azo dye applied in the textile and paper printing industries. When inhaled or ingested, it can cause eye, skin, and digestive problems (Benkhaya et al., 2020). Also, it has been observed that MR dye in high concentrations in the water may be harmful to aquatic life (Samsami et al., 2020). Hence, it is vital to remediate wastewater sources containing MR dyes.

Trifi et al. (2019) employed orange peel-derived non-AC to remove MR from aqueous systems. A quadratic polynomial mathematical modelling was used to analyse surface morphology and determine the best assessment conditions using the Doehlert model (Czyrski and Jarzebski, 2020). The pH and stirring time significantly influenced azo dye adsorption, whereas the adsorbent dosage had a negligible impact. The research findings revealed a normal distribution behaviour when analysed.

Ravindran at el. (2018) investigated the absorption of MR dye using a cassava peel NaOH-AC. The effects of dye concentration, feed flow rate, and adsorbent bed height on adsorption capacity were studied while maintaining a normal pH and temperature range of 28–31 °C. Thomas and Yoon-Nelson models with R^2 values of 0.90 were utilized

Table 3

Methylene orange dye removal from textile effluent by agricultural waste as an absorbent.

Adsorbent	Activating agent	Adsorption rate (mg/g)	Efficiency (%)	Best Isothermal model	Best Kinetic model	Reference
Pomelo peel	H_3PO_4	141	94.6	Freundlich	PSO	(Zhang et al., 2020)
	KOH	680	-	Langmuir		(Li et al., 2016)
Acacia mangium wood	KOH	181	90.5	–	PSO	(Danish and Ahmad, 2018)
Walnut peels	$ZnCl_2$	180	95	Langmuir	PSO	(Hajialigol and Masoum, 2019)
Thapsia transtagana stems	–	118.10	91.4	Langmuir	PSO	(Machrouhi et al., 2019)
Watermelon rind	H_2SO_4	27	85	Langmuir	PSO	(Üner et al., 2016) (Bhattacharjee et al., 2020a)
Coffee ground waste	–	658	–	Freundlich	PSO	(Rattanapan et al., 2017)
Wheat straw	–	304.2	–	Langmuir	PSO	(Senthil and Lee, 2020)
Pisum sativum peels	Fe_3O_4	–	96	–	–	(Prasad et al., 2017)
Rambutan peels	ZnO	–	84	–	–	(Reza et al., 2020)
Shaddock peels		94.6	54.25	Freundlich	PSO	(Tao et al., 2019)

to validate the experimental data. It was discovered that the adsorption capacity increased when the feed concentration and flow rate were raised while the carbon bed height was decreased. With a feed concentration of 200 mg/L, a flow rate of 13 ml/min, and a bed height of 20 cm, the ideal adsorption capacity of 206 mg/g was achieved.

Tay et al. (2021) produced AC through carbonization and activation of crude oil palm empty fruit bunches (EFBs). The Taguchi method was used to discover the optimal parameters for dye removal. The contribution of each factor to the reduction of MR by raw EFB and EFB-based AC was assessed. Agitation speed has the highest contribution percentage for raw EFB. Regarding EFB-based AC, the amount of adsorbent is the most crucial variable. The optimal operating parameters for raw EFB were 25 ppm of initial dye concentration, 0.01 g of adsorbent, and 200 rpm agitation speed. In contrast, for EFB-based AC, the optimal operating parameters were 20 ppm of initial dye concentration, 0.06 g of adsorbent, and 120 rpm of agitation speed. The anticipated percentages of dye removal for raw EFB (55.54%) and EFB-based AC (86.72%) were in excellent agreement with the experimental values for raw EFB (50.5%) and EFB-based AC (84.61%), respectively.

The experiments that utilized agricultural material for MR removal are included in Table 4.

2.4. Other dyes

Manihot esculenta (cassava) peels were used to produce AC, which was then thermally treated with acid, base, and silver nitrate to remove a variety of dyes (acidic, alkaline, direct, sulfuric, and reactive)

(Parvathi et al., 2018). AgNO₃-AC produced the best performance, with approximately 90% removal efficiency. Notwithstanding, the removal rate of the dyes followed the order alkalic > direct > sulfuric > acidic > reactive; the equilibrium time for direct, sulfuric, and reactive dyes at the optimal adsorbent dose of 150 mg/150 ml was 150 min, whereas it was 180 min for acidic and alkalic dyes. The removal efficiency of direct and acidic dyes improved as pH increased, whereas the opposite was found for basic and sulfuric dyes; the conductivity of the reactive dye was undetermined.

Emerald green dye was extracted by synthesizing *Musa acuminate* peels (a type of banana) and *Solanum tuberosum* (potato) (Rehman et al., 2019). At their optimal efficiency, *Musa acuminate* showed a higher adsorption capacity (10.75 mg/g) than *Solanum tuberosum* (2.61 mg/g). The Langmuir model was preferable to the Freundlich model in describing the adsorption isotherm; meanwhile, the adsorption kinetics fitted the PSO model. Maximum removal efficiencies of 96% for *Solanum tuberosum* and 76% for *Musa acuminate* were achieved at pH levels 3 and 6, respectively. However, increasing the contact time and temperature showed minor positive and negative impacts on adsorption capacity. Adsorption was the highest during short contact times. It was demonstrated that the adsorption of the cationic dye was due to the acidic functional groups of carboxyl and hydroxyl, as well as the peel powder porosity.

Citrullus lanatus peels (watermelon) were found to be effective for removing acidic dyes of eosin and fluorescein (Latif et al., 2019), comparing untreated, 0.1 N HNO₃-treated, and 0.1 N NaOH-treated powders. The alkali-treated peels demonstrated the maximum removal

Table 4

Methyl red dye removal from textile effluent by agricultural waste as an absorbent.

Adsorbent	Activating agent	Adsorption rate (mg/g)	Efficiency (%)	Best Isothermal model	Best Kinetic model	Reference
Orange peels	H_2SO_4	–	99	Langmuir	PSO	(Daful and Chandraratne, 2018)
Cassava peels	NaOH	206	78.62	Thomas and Yoon-Nelson	PSO	(Ravindran et al., 2018)
Fibers of banana pseudo-stem	–	–	88.5	Freundlich	PSO	(Saigl and Ahmed, 2021)
Potato peels	KOH	30.48	64	Freundlich	PSO	(Naik et al., 2019)
Durian seeds	H_3PO_4	384.62	92.5	Freundlich	PSO	(Ahmed et al., 2020)
Atemoya shell	K_2CO_3	435.25	64	Langmuir	PSO	(Khan et al., 2018)
Annona squamosa shell	–	226.9	61	Langmuir	PSO	(Khan et al., 2018)
Annona squamosa seed	–	40.48	82.81	Langmuir, Freundlich, Dubnin-Radushekevich and Temkin model	PSO	(Khan et al., 2018)

Table 5
Different dye removal from textile effluent by agricultural waste as an absorbent.

Adsorbent	Activating agent	Adsorbate	Surface area (m^2/g)	Total pore volume (cm^3/g)/ Diameter (nm)	Adsorption rate mg/g	Efficiency	Best Isothermal model	Best Kinetic model	Ref.
Watermelon rind	Microwave H_3PO_4	Eosin and safranine D	459 m^2/g	0.23	–	79	Freundlich	PSO	(Ibrahim and Maslehuddin, 2020)
Watermelon peels	–	Eosin Fluorescein dye	–	–	–	88	Langmuir	PSO	(Latif et al., 2019)
Potato peels	H_3PO_4	Emerald green	–	–	2.61	96	Langmuir	PSO	(Naik et al., 2019)
Banana peel	$ZnCl_2$	Reactive Black 5 (RB5) CR	–	–	211.8 164.6	90 90	Langmuir	PSO	(Munagapati et al., 2018)
Manihot esculenta peel	–	Acid Blue 92 Malachite green Direct Red 80 Sulfur Black 1 Magenta MB	–	–	–	–	–	–	(Parvathi et al., 2018)
Musa acuminate	–	Emerald green	–	–	10.75	–	Langmuir	PSO	(Rehman et al., 2019)
Walnut shell	Microwave	Malachite green	17 m^2/g	20.1	–	100	Langmuir	PSO	(Bode et al., 2019; Nudda et al., 2019; Zhou et al., 2019)
Mahogany sawdust	$ZnCl_2$	Blue 2B and direct green B	–	–	518	–	Langmuir	PSO	(Lee et al., 2020)
Pinewood	KOH	Astrazon blue, and Telon blue	3850	–	31.24	–	Langmuir	PSO	(Astuti et al., 2019)
Potato Stem powder Potato Leaves powder	–	Malachite green	–	–	27.0 33.3	67 75	Langmuir and Freundlich	PSO	(Bhomick et al., 2018) (Ahsan et al., 2018)
Orange peel	–	Direct Red 23 Direct Red 80	–	–	10.72 21.75	92 91	Langmuir	PSO	(Lei, 2018)

10

efficiency, whereas the untreated peels demonstrated the lowest. The kinetics of adsorption fitted the PSO model, and the thermal analysis of the data showed that the reaction was spontaneous and exothermic. Fluorescein and eosin adsorption was described by the Freundlich and Langmuir isotherms, respectively. The removal efficiency reduced as pH raised, particularly at pH levels above 5. The highest removal rate occurred at a contact time of around 20 min and a temperature of 25 °C.

Reactive Black 5 (RB5) and Congo Red (CR) dyes were neutralized with banana peel powder (Munagapati et al., 2018). Characterizations revealed that the powder's surface was porous and contained amine, carboxyl, and hydroxyl groups, which aided in the adsorption of dyes. The equilibrium results best suited the Langmuir isotherm, where the maximal adsorption capacities of RB5 and CR at pH 3 and ambient temp were calculated to be 49.2 and 164.6 mg/g, respectively. While the PSO model best described the kinetics of adsorption for both dyes, the pseudo-first-order model was the second best. The adsorption was spontaneous and endothermic, but the desorption was accomplished using a 0.1 M NaOH aqueous solution with 90% recovery efficiency.

Munagapati et al. (2018) have studied modified banana peels as adsorbents to remove RB5 dye from aqueous solutions. The high carbon content of banana peels (due to the presence of hemicelluloses, cellulose, chlorophyll, pectin, and other low molecular weight species) makes them a suitable precursor for producing AC. Chemical amendments increase the functional group potential and number of active sites, hence enhancing their adsorption characteristics. Formaldehyde and formic acid were used to modify the chemical composition of the banana peels. At pH 3, the maximum adsorption capacity was attained at 211.8 mg/g. Langmuir > Temkin > Freundlich > Dubinin–Radushkevich were the isotherm models that best fit the experimental results. The PSO model described the kinetic data of adsorption is higher than the pseudo-first-order model. In addition, regeneration tests using a 0.1 M NaOH solution demonstrated that the modified banana peel adsorbent could be reused five times.

The adsorption of several common textile dyes, including Reactive Black 5, Reactive Yellow 84, Acid Yellow 23, and Acid Red 18, on sunflower seed hulls, were studied. The researchers examined both aminated and non-aminated seed hulls (Jóźwiak et al., 2020). The adsorption capacity of the aminated adsorbent was significantly greater than that of the non-aminated adsorbent, increasing by 1665%, 1425%, 1881%, and 2284%, respectively, for the dyes listed above. This is owing to the animation of polysaccharides of sunflower seed hull, in which the amine groups incorporated into the sorbent serve as anionic dye sorption sites. Studies of adsorption isotherms demonstrated that the Langmuir model best describes experimental data for all dyes studied. Kinetic experiments showed that the PSO model provided the best fit for all dyes.

The adsorption of CR and malachite green (MG) was investigated on biochar produced from litchi peel using a simple hydrothermal treatment and subsequent activation (Wu et al., 2020). The adsorption rate for CR and green malachite was 404.4 mg/g and 2468 mg/g, respectively, indicating that litchi peel biochar has a high performance in adsorption. The adsorbent's specific surface area and pore volumes were 1006.0 m^2/g and 0.588.0 cm^3/g, respectively. The excellent adsorption characteristics resulted from pore filling, hydrogen bonding, - interaction, and electrostatic interactions. The Langmuir, Freundlich, Temkin, and Dubinin-Radushkevich adsorption isotherm models were investigated for CR and green malachite dyes. It was determined that the Freundlich model best described the experimental results for both dyes, suggesting that adsorption proceeded on a multilayer and heterogeneous surface.

Bhattacharjee et al. (2020b) investigated the removal of CR dye from wastewater via WMR and achieved beneficial outcomes. The authors determined that physisorption dominated the biosorption using five different isotherm models, including Langmuir, Temkin, Freundlich, Dubinin-Radushkevich, and Harkins-Jura of CR into WMR. Masoudian et al. (2019) also examined ultrasound-assisted biosorption of CR utilizing WMR containing titanium dioxide (TiO$_2$) nanoparticles.

Loading TiO$_2$ nanoparticles into the WMR, an adsorbent with a high surface area (667.8 m^2/g) was obtained. The authors conducted a response surface methodology-based experimental design using a desirability function. They reported the following optimal conditions: CR at a pH of 4.3, 0.04 g adsorbent, 8.22 min of sonication, and an initial concentration of 14.7 mg/L. It was observed that the maximum adsorption capability was 17 mg/g. Masoudian et al. (2019) also conducted desorption investigations with NaOH and discovered that the nanoparticle-loaded adsorbent was reusable for up to 5 cycles with an adsorption capacity of more than 70%. Isotherm research and biosorption process kinetic analyses indicated the Langmuir model and PSO. Thus, the researchers discovered that WMR might be employed as an inexpensive adsorbent for CR removal from wastewater.

Sahoo (2021) integrated WMR as an adsorbent to remove the anthraquinone dye Remazol Brilliant Blue Reactive (RBBR) from an aqueous system. The authors chemically activated the carbonaceous rind with KOH. The findings demonstrated that a high initial dye concentration required a substantially extended period to obtain the same adsorption percentage, which is associated with the adsorbent's active surface sites being saturated. As RBBR is an anionic dye, electrostatic interaction between the anionic dye and the positively charged surface of the melon rind led to increased adsorption at a pH of 2. The removal efficiency decreased as the pH of the solution increased. Bello et al. (2019) found comparable results for RBBR removal utilizing cocoa pod husk as an adsorbent. The authors discovered that the biosorption process was endothermic, indicating a higher adsorption rate at higher temperatures, which was compatible with Slama et al. (2021) and Zhou et al. (2019) for RBBR removal using various adsorbents. Film and intraparticle diffusion were discovered to be the predominant biosorption mechanism for RBBR. In addition, the researchers observed that the Freundlich model adequately characterized equilibrium adsorption data and that the RBBR adsorption onto WMR adsorbent followed a physisorption process.

Idrus and Hamad (2022) investigated the effectiveness of WMR in removing brilliant green (BG) dye from an aqueous solution. The investigators activated WMR using orthophosphoric acid (H$_3$PO$_4$) and discovered that activated WMR had a considerably better biosorption capacity than untreated WMR. With reported values of 32.7 and 22.6 mg/g, the researchers concluded that H$_3$PO$_4$ as an activating agent was highly effective at enhancing the adsorption capacities of WMR. The SEM analysis was carried out to study the surface morphology of WMR. The surface area of the H$_3$PO$_4$-activated WMR was three times larger than that of the raw WMR. The authors also found an increased pore volume following SEM analysis of the activated WMR. In addition, the authors noted that the biosorption equilibrium data followed the Langmuir isotherm model and that the process was exothermic and spontaneous.

Chigbundu Kayode and Adebowale (2017) studied watermelon shells as a biosorbent for the removal of the dyes Basic red 2 (BR2) and Orange G (OG) from an aqueous system. They analysed fractal-like kinetics (which contains time dependence of biosorption rate coefficients) for the biosorption process and determined that chemical reactions at the solid/solution interface were the predominant interaction mechanism between the dyes and biosorbent. Likewise, Aguilar-Rosero et al. (2022) reported similar findings. Chigbundu Kayode and Adebowale (2017) discovered that the Fractal-like pseudo-first-order kinetic equation was appropriate for interpreting kinetic data for both dyes. The chemisorptive nature of the interaction between the dyes and the active sites of the biosorbent was further validated using two-parameter models, such as the Elovich model. The authors observed that the Elovich model was appropriate for the cationic dye (BR2). In contrast, the Diffusion-Chemisorption model adequately explained the equilibrium results for the anionic dye Orange G. BR2 adsorption was endothermic, but OG adsorption was exothermic, as determined by thermodynamic analysis.

Ibrahim and Maslehuddin (2020) investigated the biosorption of MO, and Rhodamine B (RB) on WMR activated with H$_2$SO$_4$. They

discovered that dye adsorption increased with rising temperature, reaching a maximum of 318 K. The authors ascribed this response to the elimination of solvent (water) molecules, which made more active sites available at the interface. Ahmed et al. (2016) discovered a similar effect of temperature during the biosorption of RB utilizing sugarcane bagasse. Kinetic studies revealed that the PSO model applied to the absorption process and that intra-particle diffusion played a substantial role. The presence of OH^- ions at high pH promotes competition between $-N^+$ and $-COO$, reducing the aggregation of RB aggregation and causing RB adsorption at higher pH.

Zhou et al. (2020) employed an MV pyrolysis technique to synthesize biochar from agricultural residues to remove eosin and safranine D by absorption. The pore volume and biochar surface area were measured as $0.23\,cm^3/g$ and $459\,m^2/g$, respectively. Zhang et al. (2018) used a liquefaction mechanism with aqueous solutions, including ethanol, methanol, and acetone at 260–380 °C to produce biochar, which was then used to adsorb MG and MB. Although this biochar's surface area and pore size were less than those observed for carbon ($12-17\,m^2/g$ and 18.1–20.1 nm, respectively), the substance was stated to have a high concentration of oxygen functionalities. Lately, thermal alkaline pre-treatment has been employed to develop biochar for the sorption of cationic red X-GRL (Xiao et al., 2018). This technique enhanced the biochar's pore volume and surface area by 33.3% and 43.5%, respectively, resulting in a 49.2% improvement in dye removal yield, with an absorption ability of 39.1–47.6 mg/g. Lian et al. (2016) reported composing $SrFe_{12}O_{19}$ assembled magnetic biochar and its use in the removal of MG. The adsorption ability was 388.65 mg/g for an initial concentration of MG of 500 mg/L and a biomass dose of 2.0 g/L.

Hajialigol and Masoum (2019) synthesized and successfully used *Juglans regia* (walnut) shell-based AC as a biomass material to remove MG from a solvent. The effect of operating variables, particularly initial MG concentration (16.5–33.5 mg/L), nano biomass dosage (16.5–33.4 mg), and residence time (13–47 min) on MG uptake from the liquid phase, was investigated using a central composite design. About 100% removal was achieved at an initial concentration of 33.3 mg/L MG, a nano biomass dose of 33.3 mg, and a residence time of 20.0 min. When comparing the degree of MG removal at 100 mg/L concentrations, it was discovered that the nano biomass AC had the greatest extent of MG removal. As opposed to the raw walnut shell, nano biomass AC contains porous nature, well-distributed internal pore structure, and large surface area. Since nanoparticles have a large surface area in a constant volume of dye solution, more interaction between nano biomass and dye molecules could explain the effect of higher nano biomass dosage on MG removal. It was also noticeable that as the MG concentration increases, the percentage of MG removed decreases due to a reduction in the dye molecule to accessible surface adsorption sites ratio. The data was analysed using various adsorption isotherms, including Langmuir, Temkin, Freundlich, and Dubinin–Kaganer–Radushkevich (DKR), with the outcomes establishing the Langmuir isotherm as a valid model for defining adsorption behaviours. Ultimately, the PSO kinetic model accurately predicted the MG sorption mechanism ($R^2 = 0.9897$). Table 5 displays the removal of various dyes from various biomass sources.

3. Conclusions

Extensive synthesization of agricultural residue for eliminating dyes from textile effluent pollution was reviewed. This study provides an overview of the different novel absorbers from agricultural by-products (mainly peels, leaves, and seeds). It gives a general overview of removing other dyes from wastewater simulated by absorption technology. The natural atmosphere synthesizing carbon is the most abundant economic resource. The assessment also indicated that the absorption capacity of the carbon was upgraded by expanding the surface area but indicated a slight enhancement in increasing the pore size. The relationship between methyl dyes and the surface of carbon

materials was complex. Each of these technologies has its advantages and disadvantages. The transformation of adsorbent technologies is a simple, reliable, and cost-effective process that has been explored for textile effluent treatment. Thus, the decolorization of colored pollutants from wastewaters using agriculturally derived AC and biochar has shown promising results with the highest efficiency in the field of adsorption technology, as they exhibit exceptional removal capabilities for a wide variety of dye classes and could be used in place of industrial adsorbents.

Data Availability

No data was used for the research described in the article.

Declaration of Competing Interest

The authors declare that they have no known competing financial interests or personal relationships that could have appeared to influence the work reported in this paper.

Acknowledgements

References

Abdullah, M.F., Azfaralariff, A., Lazim, A.M., 2018. Methylene blue removal by using pectin-based hydrogels extracted from dragon fruit peel waste using gamma and microwave radiation polymerization techniques. J. Biomater. Sci., Polym. Ed. 29 (14), 1745–1763. https://doi.org/10.1080/09205063.2018.1489023

Aguilar-Rosero, J., Urbina-López, M.E., Rodríguez-González, B.E., León-Villegas, S.X., Luna-Cruz, I.E., Cárdenas-Chávez, D.L., 2022. Development and characterization of bioadsorbents derived from different agricultural wastes for water reclamation: a review. Appl. Sci. 12, 2740.

Ahmed, S., Aktar, S., Zaman, S., Jahan, R.A., Bari, M.L., 2020. Use of natural bio-sorbent in removing dye, heavy metal and antibiotic-resistant bacteria from industrial wastewater. Appl. Water Sci. 10 (5), 1–11. https://doi.org/10.1007/s13201-020-01200-8

Ahsan, M.A., Katla, S.K., Islam, M.T., Hernandez-Viezcas, J.A., Martinez, L.M., Díaz-Moreno, C.A., Noveron, J.C., 2018. Adsorptive removal of methylene blue, tetracycline and Cr(VI) from water using sulfonated tea waste. Environ. Technol. Innov. 11, 23–40. https://doi.org/10.1016/J.ETI.2018.04.003

Allafchian, A., Mousavi, Z.S., Hosseini, S.S., 2019. Application of cress seed musilage magnetic nanocomposites for removal of methylene blue dye from water. Int. J. Biol. Macromol. 136, 199–208. https://doi.org/10.1016/J.IJBIOMAC.2019.06.083

Amalina, F., Abd Razak, A.S., Krishnan, S., Zularisam, A.W., Nasrullah, M., 2022a. A review of eco-sustainable techniques for the removal of Rhodamine B dye utilizing biomass residue adsorbents. Phys. Chem. Earth Parts A/B/C 128, 103267. https://doi.org/10.1016/J.PCE.2022.103267

Amalina, F., Haziq, M., Syukor, A., Razak, A., Huwaida, N., Zamani, A., Hamid, A., 2019. Development of animal feed from waste to wealth using napier grass and palm acid oil (PAO) from palm oil mill effluent (POME). Mater. Today Proc. 19, 1618–1627. https://doi.org/10.1016/j.matpr.2019.11.190

Amalina, F., Syukor, A., Razak, A., Krishnan, S., Sulaiman, H., Zularisam, A.W., Nasrullah, M., 2022b. Biochar production techniques utilizing biomass waste-derived materials and environmental applications – a review. J. Hazard. Mater. Adv. 7, 100134. https://doi.org/10.1016/j.hazadv.2022.100134

Amalina, F., Syukor, A., Razak, A., Krishnan, S., Zularisam, A.W., Nasrullah, M., 2022c. A comprehensive assessment of the method for producing biochar, its characterization, stability, and potential applications in regenerative economic sustainability – a review. Clean. Mater. 3, 100045. https://doi.org/10.1016/j.clema.2022.100045

Amalina, F., Syukor, A., Razak, A., Krishnan, S., Zularisam, A.W., Nasrullah, M., 2022d. Water hyacinth (Eichhornia crassipes) for organic contaminants removal in water – A review. J. Hazard. Mater. Adv. 7, 100092. https://doi.org/10.1016/j.hazadv.2022.100092

Amalina, F., Syukor Abd Razak, A., Krishnan, S., Sulaiman, H., Zularisam, A.W., Nasrullah, M., 2022e. Advanced techniques in the production of biochar from lignocellulosic biomass and environmental applications. Clean. Mater. 6, 100137. https://doi.org/10.1016/j.clema.2022.100137

Amalina, F., Syukor Abd Razak, A., Krishnan, S., Zularisam, A.W., Nasrullah, M., 2022f. The effects of chemical modification on adsorbent performance on water and wastewater treatment - a review. Bioresour. Technol. Rep. 101259. https://doi.org/10.1016/j.biteb.2022.101259

Amalina, I.F., Haziq, J.M., Syukor, A.R.A., Rashid, A.H.M., 2020. Formulation of Capra hircus Feed to Utilize Artocarpus heterophyllus Leaves and Palm Acid Oil (PAO). IOP Conf. Ser. Mater. Sci. Eng. 763 (022016), 1–7. https://doi.org/10.1088/1757-899X/736/2/022016

Amalina, I.F., Haziq, J.M., Syukor, A.R.A., Ridwan, A.F.A., Rashid, A.H.M., 2021. Study of Palm Acid Oil (PAO) from Sludge Palm Oil Mill Effluent (POME) as Goat ' s Feed. Mater. Today.: Proc. 41, 96–101. https://doi.org/10.1016/j.matpr.2020.11.1013

Ansari, S.A., Khan, F., Ahmad, A. (2016). Cauliflower Leave, an Agricultural Waste Biomass Adsorbent, and Its Application for the Removal of MB Dye from Aqueous Solution: Equilibrium, Kinetics, and Thermodynamic Studies. https://doi.org/10.1155/2016/8252354.

Astuti, W., Sulistyaningsih, T., Kusumastuti, E., Yanny, G., Sari, R., 2019. Bioresource technology thermal conversion of pineapple crown leaf waste to magnetized activated carbon for dye removal. Bioresour. Technol. 287, 121426. https://doi.org/10.1016/j.biortech.2019.121426

Bagotia, N., Sharma, A.K., Kumar, S., 2020. Jo ur na l P re of. ECSN, 129309. https://doi.org/10.1016/j.chemosphere.2020.129309

Bedia, J., Peñas-Garzón, M., Gómez-Avilés, A., Rodriguez, J., Belver, C., 2018. A review on the synthesis and characterization of biomass-derived carbons for adsorption of emerging contaminants from water. C 4 (4), 63. https://doi.org/10.3390/c4040063

Bello, O.S., Adegoke, K.A., Sarumi, O.O., Lameed, O.S., 2019. Functionalized locust bean pod (Parkia biglobosa) activated carbon for Rhodamine B dye removal. Heliyon 5 (8), 02323. https://doi.org/10.1016/j.heliyon.2019.e02323

Benkhaya, S., Souad, M., Harfi, A.El, 2020. A review on classifications, recent synthesis and applications of textile dyes. Inorg. Chem. Commun. 115, 107891. https://doi.org/10.1016/j.inoche.2020.107891

Bhattacharjee, C., Dutta, S., Saxena, V.K., 2020a. A review on biosorptive removal of dyes and heavy metals from wastewater using watermelon rind as biosorbent. Environ. Adv. 2, 100007. https://doi.org/10.1016/j.envadv.2020.100007

Bhattacharjee, C., Dutta, S., Saxena, V.K., 2020b. A review on biosorptive removal of dyes and heavy metals from wastewater using watermelon rind as biosorbent. Environ. Adv. 2, 100007. https://doi.org/10.1016/j.envadv.2020.100007

Bhomick, P.C., Supong, A., Baruah, M., Pongener, C., 2018. Pine Cone biomass as an e ffi cient precursor for the synthesis of activated biocarbon for adsorption of anionic dye from aqueous solution: Isotherm, kinetic, thermodynamic and regeneration studies. Sustain. Chem. Pharm. 10, 41–49. https://doi.org/10.1016/j.scp.2018.09.001

Bode, O.O., Noah, F.A., Adebayo, A.J., 2019. Nitrogen metabolism, digestibility and blood profile of West African dwarf goats fed dietary levels of Cajanus cajan as supplement to cassava peels. J. Rangel. Sci. 9 (1), 13–23.

Chen, S., Qin, C., Wang, T., Chen, F., Li, X., Hou, H., Zhou, M., 2019. Study on the adsorption of dyestuffs with different properties by sludge-rice husk biochar: adsorption capacity, isotherm, kinetic, thermodynamics and mechanism. J. Mol. Liq. 285, 62–74. https://doi.org/10.1016/j.molliq.2019.04.035

Chigbundu Kayode O Adebowale, E.C., 2017. Equilibrium and fractal-like kinetic studies of the sorption of acid and basic dyes onto watermelon shell (Citrullus vulgaris. Nigeria123Cellulose 24, 4701–4714. https://doi.org/10.1007/s10570-017-1488-2

Czyrski, A., Jarzebski, H., 2020. Response surface methodology as a useful tool for evaluation of the recovery of the fluoroquinolones from plasma-the study on applicability of box-behnken design, central composite design and doehlert design. Processes 8 (4). https://doi.org/10.3390/PR8040473

Daful, A.G., Chandraratne, M.R., 2018. Biochar production from biomass waste-derived material. Encycl. Renew. Sustain. Mater. https://doi.org/10.1016/B978-0-12-803581-8.11249-4

Danish, M., Ahmad, T., 2018. A review on utilization of wood biomass as a sustainable precursor for activated carbon production and application. Renew. Sustain. Energy Rev. 87, 1–21. https://doi.org/10.1016/j.rser.2018.02.003

Eljiedi, A.A.A., Kamari, A., 2017. Removal of methyl orange and methylene blue dyes from aqueous solution using lala clam (Orbicularia orbiculata) shell. AIP Conf. Proc. *1847*. https://doi.org/10.1063/1.4983899

Esteves, B.M., Torres, S.M., Madeira, L.M., Maldonado-Hódar, F.J, 2020. Fitting biochars and activated carbons from residues of the olive oil industry as supports of fe-catalysts for the heterogeneous fenton-like treatment of simulated olive mill wastewater. Nanomaterials 10 (5). https://doi.org/10.3390/nano10050876

Fang, Y., Yang, K., Zhang, Y., Peng, C., Robledo-Cabrera, A., López-Valdivieso, A., 2021. Highly surface activated carbon to remove Cr(VI) from aqueous solution with adsorbent recycling. Environ. Res. 197, 111151. https://doi.org/10.1016/J.ENVRES.2021.111151

Gu, A. (2021). Removal of dyes and pigments from industrial effluents. https://doi.org/10.1016/B978-0-12-817742-6.00005-0.

Gupta, N., Kushwaha, A.K., Chattopadhyaya, M.C., 2016. Application of potato (Solanum tuberosum) plant wastes for the removal of methylene blue and malachite green dye from aqueous solution. Arab. J. Chem. 9, S707–S716. https://doi.org/10.1016/J.ARABJC.2011.07.021

Hajialigol, S., Masoum, S., 2019. Optimization of biosorption potential of nano biomass derived from walnut shell for the removal of Malachite Green from liquids solution: Experimental design approaches. J. Mol. Liq. 286, 110904. https://doi.org/10.1016/j.molliq.2019.110904

Hassan, M., Liu, Y., Naidu, R., Parikh, S.J., Du, J., Qi, F., Willett, I.R., 2020. Science of the total environment influences of feedstock sources and pyrolysis temperature on the properties of biochar and functionality as adsorbents: a meta-analysis. Sci. Total Environ. 744, 140714. https://doi.org/10.1016/j.scitotenv.2020.140714

Hassan, M.M., Carr, C.M., 2021. Chemosphere Biomass-derived porous carbonaceous materials and their composites as adsorbents for cationic and anionic dyes: A review. Chemosphere 265, 129087. https://doi.org/10.1016/j.chemosphere.2020.129087

Haziq, J.M., Amalina, I.F., Syukor, A.R.A., Islam, N., 2020. Peat swamp groundwater treatment: efficiency of mixed citrus peel and kernel activated carbon layer. IOP

Conf. Ser.: Mater. Sci. Eng. 736 (022113), 1–9. https://doi.org/10.1088/1757-899X/736/2/022113

Ibrahim, M., Maslehuddin, M., 2020. An overview of factors influencing the properties of alkali-activated binders. J. Clean. Prod., 124972. https://doi.org/10.1016/j.jclepro.2020.124972

Idrus, S., Hamad, H.N., 2022. Recent developments in the application of bio-waste-derived adsorbents for the removal of methylene blue from. Polymers 14 (783), 1–39.

Iftekhar, S., Ramasamy, D.L., Srivastava, V., Asif, M.B., Sillanpää, M., 2018. Understanding the factors affecting the adsorption of Lanthanum using different adsorbents: a critical review. Chemosphere Vol. 204, 413–430. https://doi.org/10.1016/j.chemosphere.2018.04.053

Jawad, A.H., Murtadha, A., Ngoh, Y.S., 2018. Applicability of dragon fruit (Hylocereus polyrhizus) peels as low-cost biosorbent for adsorption of methylene blue from aqueous solution: Kinetics, equilibrium and thermodynamics studies. Desalin. Water Treat. 109, 21976. https://doi.org/10.5004/dwt.2018.21976

Jawad, A.H., Razuan, R., Appaturi, J.N., Wilson, L.D., 2019. Adsorption and mechanism study for methylene blue dye removal with carbonized watermelon (Citrullus lanatus)rind prepared via one-step liquid phase H 2 SO 4 activation. Surf. Interfaces 16, 76–84. https://doi.org/10.1016/j.surfin.2019.04.012

Jesudoss, N.R., Kumar, J.S., Kamyab, H., Jennifa, J.A., Al-khashman, O.A., Kuslu, Y., Kumar, B.S., 2020. Modern enabling techniques and adsorbents based dye removal with sustainability concerns in textile industrial sector -a comprehensive review. J. Clean. Prod. 272, 122636. https://doi.org/10.1016/j.jclepro.2020.122636

Ji, B., Wang, J., Song, H., Chen, W., 2019. Removal of methylene blue from aqueous solutions using biochar derived from a fallen leaf by slow pyrolysis: Behavior and mechanism. J. Environ. Chem. Eng. 7 (3), 103036. https://doi.org/10.1016/J.JECE.2019.103036

Jinendra, U., Bilehal, D., Nagabhushana, B.M., Kumar, A.P., 2021. Adsorptive removal of Rhodamine B dye from aqueous solution by using graphene–based nickel nanocomposite. Heliyon 7 (4), e06851. https://doi.org/10.1016/j.heliyon.2021.e06851

Jóźwiak, T., Filipkowska, U., Brym, S., Kopeć, L., 2020. Use of aminated hulls of sunflower seeds for the removal of anionic dyes from aqueous solutions. Int. J. Environ. Sci. Technol. 17 (3), 1211–1224. https://doi.org/10.1007/s13762-019-02536-8

Kadhom, M., Albayati, N., Alalwan, H., Al-furaiji, M., 2020. Removal of dyes by agricultural waste. Sustain. Chem. Pharm. 16 (January), 100259. https://doi.org/10.1016/j.scp.2020.100259

Karnan, T., Selvakumar, S.A.S., 2016. Biosynthesis of ZnO nanoparticles using rambutan (Nephelium lappaceumL.) peel extract and their photocatalytic activity on methyl orange dye. J. Mol. Struct. 1125, 358–365. https://doi.org/10.1016/J.MOLSTRUC.2016.07.029

Khan, E.A., Shahjahan, Khan, T.A., 2018. Adsorption of methyl red on activated carbon derived from custard apple (Annona squamosa) fruit shell: Equilibrium isotherm and kinetic studies. J. Mol. Liq. 249, 1195–1211. https://doi.org/10.1016/j.molliq.2017.11.125

Krishnan, S., Kadier, A., Fadhil Bin, M.D., Din, M., Nasrullah, M., Najiha, N.N., Taib, S.M., Singh, L., 2021. Application of bioelectrochemical systems in wastewater treatment and hydrogen production. Deliv. Low. Carbon Biofuels Bioprod. Recovery 31–44. https://doi.org/10.1016/B978-0-12-821841-9.00003-7

Krishnan, S., Zulkapli, N.S., Kamyab, H., Taib, S.M., Din, M.F.B.M., Majid, Z.A., Othman, N., 2021. Current technologies for recovery of metals from industrial wastes: an overview. Environ. Technol. Innov. 22, 101525. https://doi.org/10.1016/j.eti.2021.101525

Labiadh, L., Kamali, A.R., 2020. Textural, structural and morphological evolution of mesoporous 3D graphene saturated with methyl orange dye during thermal regeneration. Diam. Relat. Mater. 103, 107698. https://doi.org/10.1016/j.diamond.2020.107698

Lai, K.C., Lee, L.Y., Hiew, B.Y.Z., Yang, T.C.K., Pan, G.T., Thangalazhy-Gopakumar, S., Gan, S., 2020. Utilisation of eco-friendly and low cost 3D graphene-based composite for treatment of aqueous Reactive Black 5 dye: Characterisation, adsorption mechanism and recyclability studies. J. Taiwan Inst. Chem. Eng. 114, 57–66. https://doi.org/10.1016/j.jtice.2020.09.024

Latif, S., Rehman, R., Imran, M., Iqbal, S., Kanwal, A., Mitu, L., 2019. Removal of acidic dyes from aqueous media using citrullus lanatus peels: an agrowaste-based adsorbent for environmental safety. J. Chem. https://doi.org/10.1155/2019/6704953

Lee, D.J., Lu, J.S., Chang, J.S., 2020. Pyrolysis synergy of municipal solid waste (MSW): a review. Bioresour. Technol. 318, 123912. https://doi.org/10.1016/j.biortech.2020.123912

Lei, Q. (2018). Microwave hydrothermal carbonization of orange peel waste.

Li, H., Sun, Z., Zhang, L., Tian, Y., Cui, G., Yan, S., 2016. A cost-effective porous carbon derived from pomelo peel for the removal of methyl orange from aqueous solution. Colloids Surf. A Physicochem. Eng. Asp. 489, 191–199. https://doi.org/10.1016/J.COLSURFA.2015.10.041

Li, W., Mu, B., Yang, Y., 2019. Feasibility of industrial-scale treatment of dye wastewater via bio- adsorption technology. Bioresour. Technol. 277 (January), 157–170. https://doi.org/10.1016/j.biortech.2019.01.002

Lian, F., Cui, G., Liu, Z., Duo, L., Zhang, G., Xing, B., 2016. One-step synthesis of a novel N-doped microporous biochar derived from crop straws with high dye adsorption capacity. J. Environ. Manag. 176, 61–68. https://doi.org/10.1016/j.jenvman.2016.03.043

Liu, Z., Singer, S., Tong, Y., Kimbell, L., Anderson, E., Hughes, M., McNamara, P., 2018. Characteristics and applications of biochars derived from wastewater solids. July 1. Renew. Sustain. Energy Rev. Vol. 90, 650–664. https://doi.org/10.1016/j.rser.2018.02.040

Lu, Y., Li, S., 2019. Preparation of hierarchically interconnected porous banana peel activated carbon for methylene blue adsorption. J. Wuhan. Univ. Technol., Mater. Sci. Ed. 34 (2), 472–480. https://doi.org/10.1007/s11595-019-2076-0

Mukhlish, M.Z. Bin, Khan, Maksudur Rahman, Islam, M.S., Nazir, M.I., Snigdha, J.S., Akter, R., Ahmad, H., 2020. Decolorization of reactive dyes from aqueous solution using combined coagulation-flocculation and photochemical oxidation (UV/H$_2$O$_2$. Sustain. Chem. Eng. 1 (2), 51–61. https://doi.org/10.37256/sce.122020214.51-61

Ma, L., Jiang, C., Lin, Z., Zou, Z., 2018. Microwave-hydrothermal treated grape peel as an efficient biosorbent for methylene blue removal. Int J. Environ. Res Public Health 239 (15(2)), 1–10. https://doi.org/10.3390/ijerph15020239

Machrouhi, A., Alilou, H., Farnane, M., El Hamidi, S., Sadiq, M., Abdennouri, M., Barka, N., 2019. Statistical optimization of activated carbon from Thapsia transtagana stems and dyes removal efficiency using central composite design. J. Sci. Adv. Mater. Devices 4 (4), 544–553. https://doi.org/10.1016/j.jsamd.2019.09.002

Masoudian, N., Rajabi, M., Ghaedi, M., 2019. Titanium oxide nanoparticles loaded onto activated carbon prepared from bio-waste watermelon rind for the efficient ultrasonic-assisted adsorption of congo red and phenol red dyes from wastewaters. Polyhedron 173, 114105. https://doi.org/10.1016/J.POLY.2019.114105

Mishra, S., Cheng, L., Maiti, A., 2021. The utilization of agro-biomass / byproducts for effective bio-removal of dyes from dyeing wastewater: a comprehensive review. J. Environ. Chem. Eng. 9 (1), 104901. https://doi.org/10.1016/j.jece.2020.104901

Mohamad, Z., Razak, A.A., Krishnan, S., Singh, L., Zularisam, A.W., Nasrullah, M., 2022. Treatment of palm oil mill effluent using electrocoagulation powered by direct photovoltaic solar system. Chem. Eng. Res. Des. 177, 578–582. https://doi.org/10.1016/J.CHERD.2021.11.019

Munagapati, V.S., Yarramuthi, V., Kim, Y., Lee, K.M., Kim, D.S., 2018. Removal of anionic dyes (Reactive Black 5 and Congo Red) from aqueous solutions using Banana Peel Powder as an adsorbent. Ecotoxicol. Environ. Saf. 148, 601–607. https://doi.org/10.1016/j.ecoenv.2017.10.075

Naik, B., Goyal, S.K., Tripathi, A.D., Kumar, V., 2019. Screening of agro-industrial waste and physical factors for the optimum production of pullulanase in solid-state fermentation from endophytic Aspergillus sp. Biocatal. Agric. Biotechnol. 22, 101423. https://doi.org/10.1016/j.bcab.2019.101423

Nasrullah, M., Ansar, S., Krishnan, S., Singh, L., Peera, S.G., Zularisam, A.W., 2022. Electrocoagulation treatment of raw palm oil mill effluent: optimization process using high current application. Chemosphere 299, 134387. https://doi.org/10.1016/J.CHEMOSPHERE.2022.134387

Nasrullah, M., Singh, L., Krishnan, S., Sakinah, M., Mahapatra, D.M., Zularisam, A.W., 2020. Electrocoagulation treatment of raw palm oil mill effluent: effect of operating parameters on floc growth and structure. J. Water Process Eng. 33 (December 2019), 101114. https://doi.org/10.1016/j.jwpe.2019.101114

Nasrullah, M., Zularisam, A.W., Krishnan, S., Sakinah, M., Singh, L., Fen, Y.W., 2019. High performance electrocoagulation process in treating palm oil mill effluent using high current intensity application. Chin. J. Chem. Eng. 27 (1), 208–217. https://doi.org/10.1016/j.cjche.2018.07.021

Nazir, M.A., Bashir, M.A., Najam, T., Javed, M.S., Suleman, S., Hussain, S., Rehman, A. ur, 2021. Combining structurally ordered intermetallic nodes: Kinetic and isothermal studies for removal of malachite green and methyl orange with mechanistic aspects. Microchem. J. 164, 105973. https://doi.org/10.1016/j.microc.2021.105973

Nedjai, R., Alkhatib, M.F.R., Alam, M.Z., Kabbashi, N.A., 2021. Adsorption of methylene blue onto activated carbon developed from baobab fruit shell by chemical activation: kinetic equilibrium studies. IIUM Eng. J. 22 (2), 31–49. https://doi.org/10.31436/iiumej.v22i2.1682

Nudda, A., Buffa, G., Atzori, A.S., Cappai, M.G., Caboni, P., Fais, G., Pulina, G., 2019. Small amounts of agro-industrial byproducts in dairy ewes diets affects milk production traits and hematological parameters. Anim. Feed Sci. Technol. 251 (December 2018), 76–85. https://doi.org/10.1016/j.anifeedsci.2019.02.007

Nwuzor, I.C., Chukwuneke, J.L., Nwanonenyi, S.C., Obasi, H.C., Ihekweme, G.O., 2018. Modification and Physiochemical Characterization of Kaolin Clay for Adsorption of Pollutants from Industrial Paint Effluent. Eur. J. Adv. Eng. Technol. 5 (8), 609–620.

Nyoo, J., Ju, Y., Edi, F. (2021). Biosorption of dyes. In Green Chemistry and Water Remediation: Research and Applications. https://doi.org/10.1016/B978–0–12–817742-6.00004–9.

Oliveira, F.R., Patel, A.K., Jaisi, D.P., Adhikari, S., Lu, H., Khanal, K., 2017. Environmental application of biochar: current status and perspectives. Bioresour. Technol. 246, 110–122. https://doi.org/10.1016/j.biortech.2017.08.122

Parvathi, C., Shoba, U.S., Prakash, C., Sivamani, S., 2018. Manihot esculenta peel powder: effective adsorbent for removal of various textile dyes from aqueous solutions. J. Test. Eval. 46 (6). https://doi.org/10.1520/JTE20170160

Prasad, C., Yuvaraja, G., Venkateswarlu, P., 2017. Biogenic synthesis of Fe3O4 magnetic nanoparticles using Pisum sativum peels extract and its effect on magnetic and Methyl orange dye degradation studies. J. Magn. Magn. Mater. 424, 376–381. https://doi.org/10.1016/j.JMMM.2016.10.084

Rangabhashiyam, S., Balasubramanian, P., 2019. The potential of lignocellulosic biomass precursors for biochar production: performance, mechanism and wastewater application — a review. Ind. Crops Prod. 128 (2018), 405–423. https://doi.org/10.1016/j.indcrop.2018.11.041

Rashid, J., Tehreem, F., Rehman, A., Kumar, R., 2019. Synthesis using natural functionalization of activated carbon from pumpkin peels for decolourization of aqueous methylene blue. Sci. Total Environ. 671, 369–376. https://doi.org/10.1016/j.scitotenv.2019.03.363

Raud, M., Kikas, T., Sippula, O., Shurpali, N.J., 2019. Potentials and challenges in lignocellulosic biofuel production technology. Renew. Sustain. Energy Rev. 111 (July 2018), 44–56. https://doi.org/10.1016/j.rser.2019.05.020

Ravindran, R., Hassan, S.S., Williams, G.A., Jaiswal, A.K., 2018. A review on bioconversion of agro-industrial wastes to industrially important enzymes. Bioengineering 5 (4), 1–20. https://doi.org/10.3390/bioengineering5040093

Rawat, A.P., Kumar, V., Devendra, Singh, P., Singh, D.P., 2019. A combined effect of adsorption and reduction potential of biochar derived from Mentha plant waste on removal of methylene blue dye from aqueous solution A combined effect of adsorption and reduction potential of biochar derived from Mentha plant waste on. Sep. Sci. Technol. 55 (5), 907–921. https://doi.org/10.1080/01496395.2019.1580732

Rehman, R., Farooq, S., Mahmud, T., 2019. Use of Agro-waste Musa acuminata and Solanum tuberosum peels for economical sorptive removal of Emerald green dye in ecofriendly way. J. Clean. Prod. 206, 819–826. https://doi.org/10.1016/j.jclepro.2018.09.226

Ren, Y., Ren, Y., Yang, W., Tang, X., Wu, F., Wu, Q., 2018. Comparison for younger and older adults: stimulus temporal asynchrony modulates audiovisual integration. Int. J. Psychophysiol. 124 (March 2017), 1–11. https://doi.org/10.1016/j.ijpsycho.2017.12.004

Reza, M.S., Yun, C.S., Afroze, S., Radenahmad, N., Bakar, M.S.A., Saidur, R., Azad, A.K., 2020. Preparation of activated carbon from biomass and its' applications in water and gas purification, a review. Arab J. Basic Appl. Sci. 27 (1), 208–238. https://doi.org/10.1080/25765299.2020.1766799

Roik, N.V., Belyakova, L.A., Dziazko, M.O., 2021. Selective sorptive removal of Methyl Red from individual and binary component solutions by mesoporous organosilicas of MCM-41 type. J. Environ. Sci. 99, 59–71. https://doi.org/10.1016/j.jes.2020.04.027

Sahoo, J.K., 2021. Removal of dyes using various organic peel-based materials: a systematic review. Lett. Appl. NanoBioScience 11 (3), 3714–3727. https://doi.org/10.33263/lianbs113.37143727

Sahu, S., Pahi, S., Sahu, J.K., Sahu, U.K., Patel, R.K., 2020. Kendu (Diospyros melanoxylon Roxb) fruit peel activated carbon—an efficient bioadsorbent for methylene blue dye: equilibrium, kinetic, and thermodynamic study. Environ. Sci. Pollut. Res. 27 (18), 22579–22592. https://doi.org/10.1007/s11356-020-08561-2

Said, A., Tekasakul, S., Phoungthong, K., 2020. Investigation of hydrochar derived from male oil palm flower: characteristics and application for dye removal. Pol. J. Environ. Stud. 29 (1), 807–816. https://doi.org/10.15244/pjoes/103355

Saigl, Z.M., Ahmed, A.M., 2021. Separation of rhodamine b dye from aqueous media using natural pomegranate peels. Indones. J. Chem. 21 (1), 212–224. https://doi.org/10.22146/ijc.58592

Samsami, S., Mohamadi, M., Rene, E.R., Firoozbahr, M., 2020. Recent advances in the treatment of dye-containing wastewater from textile industries: overview and perspectives. Process Saf. Environ. Prot. 143, 138–163. https://doi.org/10.1016/j.psep.2020.05.034

Senthil, C., Lee, C.W., 2020. Biomass-derived biochar materials as sustainable energy sources for electrochemical energy storage devices. Renew. Sustain. Energy Rev. (xxxx), 110464. https://doi.org/10.1016/j.rser.2020.110464

Shakoor, S., Nasar, A., 2017. Adsorptive treatment of hazardous methylene blue dye from artificially contaminated water using Cucumis sativus peel waste as a low-cost adsorbent. Groundw. Sustain. Dev. 5, 152–159. https://doi.org/10.1016/J.GSD.2017.06.005

Shamsollahi, Z., Partovinia, A., 2019. Recent advances on pollutants removal by rice husk as a bio-based adsorbent: a critical review. J. Environ. Manag. 246, 314–323. https://doi.org/10.1016/j.jenvman.2019.05.145

Singh, J.K., Chaurasia, B., Dubey, A., Manuel, A., Noguera, F., Gupta, A., Hashem, A. (2021). Biological Characterization and Instrumental Analytical Comparison of Two Biorefining Pretreatments for Water Hyacinth (Eicchornia crassipes) Biomass Hydrolysis.

Slama, H.Ben, Bouket, A.C., Pourhassan, Z., Alenezi, F.N., Silini, A., Cherif-Silini, H., Belbahri, L., 2021. Diversity of synthetic dyes from textile industries, discharge impacts and treatment methods. Appl. Sci. (Switz.) 11 (14), 1–21. https://doi.org/10.3390/app11146255

Soto-Robles, C.A., Nava, O.J., Vilchis-Nestor, A.R., Castro-Beltrán, A., Gómez-Gutiérrez, C.M., Lugo-Medina, E., Luque, P.A., 2017. Biosynthesized zinc oxide using Lycopersicon esculentum peel extract for methylene blue degradation. J. Mater. Sci. Mater. Electron. 29, 3722–3729. https://doi.org/10.1007/s10854-017-8305-4

Stjepanovi, M., Gali, A., Kosovi, I., Jakovljevi, T., Habuda-stani, M., 2021. From waste to biosorbent: removal of congo red from water. Water 13 (279), 1–17.

Rattanapan, Supaporn, Srikram, Jiraporn, kongsune, P., 2017. Adsorption of methyl orange on coffee grounds activated carbon. Energy Procedia 138, 949–954. https://doi.org/10.1016/j.egypro.2017.10.064

Tao, X., Wu, Y., Cha, L., 2019. Shaddock peels-based activated carbon as cost-saving adsorbents for efficient removal of Cr (VI) and methyl orange. Environ. Sci. Pollut. Res. 26 (19), 19828–19842. https://doi.org/10.1007/s11356-019-05322-8

Tay, W.Y., Ng, L.Y., Ng, C.Y., Sim, L.C., 2021. Removal of methyl red using adsorbent produced from empty fruit bunches by Taguchi approach. IOP Conf. Ser. Earth Environ. Sci. 945 (1). https://doi.org/10.1088/1755-1315/945/1/012014

Thomas, P., Lai, C.W., Rafie, M., Johan, B., 2019. Journal of analytical and applied pyrolysis recent developments in biomass-derived carbon as a potential sustainable material for super-capacitor-based energy storage and environmental applications. J. Anal. Appl. Pyrolysis 140, 54–85. https://doi.org/10.1016/j.jaap.2019.03.021

Tkaczyk, A., Mitrowska, K., Posyniak, A., 2020. Science of the total environment synthetic organic dyes as contaminants of the aquatic environment and their implications for ecosystems: a review. Sci. Total Environ. 717, 137222. https://doi.org/10.1016/j.scitotenv.2020.137222

Trifi, B., Bouallegue, M.C., Marzouk Trifi, I., 2019. Application of response surface methodology for optimization of methyl red adsorption by orange peels. Desalin. Water Treat. 154, 369–375. https://doi.org/10.5004/dwt.2019.24086

Üner, O., Geçgel, Ü., Bayrak, Y., 2016. Adsorption of methylene blue by an efficient activated carbon prepared from citrullus lanatus rind: kinetic, isotherm, thermodynamic, and mechanism analysis. Water Air Soil Pollut. 227 (7). https://doi.org/10.1007/s11270-016-2949-1

Wahi, R., Fakhirah, N., Yusof, Y., Jamel, J., Kanakaraju, D., Ngaini, Z., 2017. Biomass and bioenergy chemically treated microwave-derived biochar: an overview. Biomass Bioenergy. https://doi.org/10.1016/j.biombioe.2017.08.007

Wang, X., Baker, J., Carlson, K., Li, Z., 2022. Mechanisms of selected anionic dye removal by clinoptilolite. Crystals 12 (5), 1–16. https://doi.org/10.3390/cryst12050727

Wijaya, R., Andersan, G., Permatasari Santoso, S., Irawaty, W., 2020. Green reduction of graphene oxide using Kaffir Lime peel extract (Citrus hystrix) and its application as adsorbent for methylene blue. Sci. Rep. https://doi.org/10.1038/s41598-020-57433-9

Wu, J., Yang, J., Feng, P., Huang, G., Xu, C., Lin, B., 2020. High-efficiency removal of dyes from wastewater by fully recycling litchi peel biochar. Chemosphere 246, 125734. https://doi.org/10.1016/J.CHEMOSPHERE.2019.125734

Xiang, W., Zhang, X., Chen, J., Zou, W., He, F., Hu, X., Gao, B., 2020. Biochar technology in wastewater treatment: a critical review. Chemosphere Vol. 252, 126539. https://doi.org/10.1016/j.chemosphere.2020.126539

Xiao, B., Dai, Q., Yu, X., Yu, P., Zhai, S., Liu, R., Chen, H., 2018. Effects of sludge thermal-alkaline pretreatment on cationic red X-GRL adsorption onto pyrolysis biochar of sewage sludge. J. Hazard. Mater. 343, 347–355. https://doi.org/10.1016/j.jhazmat.2017.10.001

Yaashikaa, P.R., Kumar, P.S., Varjani, S.J., Saravanan, A., 2019. Advances in production and application of biochar from lignocellulosic feedstocks for remediation of environmental pollutants. Bioresour. Technol. 292, 122030. https://doi.org/10.1016/j.biortech.2019.122030

Yoneda, J.S., de Araujo, D.R., Sella, F., Liguori, G.R., Liguori, T.T.A., Moreira, L.F.P., Itri, R., 2021. Self-assembled guanosine-hydrogels for drug-delivery application: Structural and mechanical characterization, methylene blue loading and controlled release. Mater. Sci. Eng. C. 121, 111834. https://doi.org/10.1016/j.msec.2020.111834

Zaied, B.K., Rashid, M., Nasrullah, M., Zularisam, A.W., Pant, D., Singh, L., 2020. A comprehensive review on contaminants removal from pharmaceutical wastewater by electrocoagulation process. Sci. Total Environ. 726, 138095. https://doi.org/10.1016/j.scitotenv.2020.138095

Zhang, Haipeng, Xu, F., Xue, J., Chen, S., Wang, J., Yang, Y., 2020. Enhanced removal of heavy metal ions from aqueous solution using manganese dioxide-loaded biochar: Behavior and mechanism. Sci. Rep. 10 (1), 1–14. https://doi.org/10.1038/s41598-020-63000-z

Zhang, He, Xue, G., Chen, H., Li, X., 2018. Magnetic biochar catalyst derived from biological sludge and ferric sludge using hydrothermal carbonization: Preparation, characterization and its circulation in Fenton process for dyeing wastewater treatment. Chemosphere 191, 64–71. https://doi.org/10.1016/j.chemosphere.2017.10.026

Zhou, J., Jiang, Z., Qin, X., Zhang, L., 2020. Efficiency of Pb, Zn, Cd and Mn removal from Karst water by Eichhornia crassipes. Int. J. Environ. Res. Public Health 17 (5329), 16 https://doi.org/https://doi:10.3390/ijerph17155329.

Zhou, Y., Lu, J., Zhou, Y., Liu, Y., 2019. Recent advances for dyes removal using novel adsorbents: a review. Environ. Pollut. 252, 352–365. https://doi.org/10.1016/j.envpol.2019.05.072

Zhu, S., Huang, X., Wang, D., Wang, L., Ma, F., 2018. Enhanced hexavalent chromium removal performance and stabilization by magnetic iron nanoparticles assisted biochar in aqueous solution: mechanisms and application potential. Chemosphere 207, 50–59. https://doi.org/10.1016/j.chemosphere.2018.05.046

Zubair, M., Ihsanullah, I., Abdul Aziz, H., Azmier Ahmad, M., Al-Harthi, M.A., 2021. Sustainable wastewater treatment by biochar/layered double hydroxide composites: progress, challenges, and outlook. Bioresour. Technol. Vol. 319, 124128. https://doi.org/10.1016/j.biortech.2020.124128